Acidity and o-xylene isomerization activity of silica-alumina catalysts
by Johnny Lealen Golden

A thesis submitted in partial fulfillment of the requirements for the degree of Doctor of Philosophy in Chemical Engineering
Montana State University
© Copyright by Johnny Lealen Golden (1986)

Abstract:
Surface heterogeneity of a catalyst can be described in terms of adsorption energy distribution. In the present study, acid-site adsorption energy distributions have been obtained for the amorphous silica-alumina system, with results compared to o-xylene isomerization activity.

Xerogels ranging in composition from pure silica to pure alumina were synthesized using reagents which avoid sodium contamination. Calcination at 500°C was performed prior to making physical property, chemisorption, and activity measurements.

Catalysts were tested for surface area, porosity, density, alumina content, and water loss. Results indicate that unusual materials have been synthesized in the 50-75% alumina composition range, materials with low surface areas despite having high initial water contents.

Triethylamine chemisorption isotherms were gravimetrically measured at □300°C. The minimum adsorbate injection possible with the equipment used was not low enough to measure the very low coverage portion of the isotherms. The adsorption isotherms were analyzed with a recently-developed numerical technique known as CAEDMON (Computed Adsorption Energy Distribution in the MONolayer). The calculated quantities of strong acid sites for test catalysts was in general agreement with other chemisorption studies on comparable materials.

Catalyst activity for o-xylene isomerization was measured at 300-400°C using a Berty reactor. Reaction rates were obtained avoiding equilibrium and transport limitations. Activation energies of 17 to 21 kcal/mole were observed for reactive catalysts.

Reaction rates for low alumina-content catalysts were observed to be exponentially related to the quantity of strong acid-sites. Correction of intermediate alumina content catalysts for alumina-type acidity unreactive for o-xylene isomerization yielded acidities fitting the exponential relationship.

It is postulated that two major types of strong acid sites were observed for the silica-alumina catalysts, Bronsted acid sites active for isomerization and Lewis acid sites associated with alumina which are inactive for isomerization. The exponential relationship between the quantity of Bronsted sites and catalytic activity appears to indicate a proximity effect, such that acid-site reactivity increases as the distance between acid sites decreases.

ACIDITY AND o-XYLENE ISOMERIZATION ACTIVITY OF SILICA-ALUMINA CATALYSTS

by

Johnny Lealen Golden

A thesis submitted in partial fulfillment
of the requirements for the degree

of

Doctor of Philosophy

in

Chemical Engineering

MONTANA STATE UNIVERSITY
Bozeman, Montana

August 1986

MAIN LIB.
D378
G566
Cop. 2

APPROVAL

of a thesis submitted by

Johnny Lealen Golden

This thesis has been read by each member of the thesis committee and has been found to be satisfactory regarding content, English usage, format, citations, bibliographic style, and consistency, and is ready for submission to the College of Graduate Studies.

June 16, 1986
Date

John T. Sears
Chairperson, Graduate Committee

Approved for the Major Department

June 16, 1986
Date

John T. Sears
Head, Major Department

Approved for the College of Graduate Studies

August 25, 1986
Date

Henry L. Parsons
Graduate Dean

STATEMENT OF PERMISSION TO USE

In presenting this thesis in partial fulfillment of the requirements for a doctoral degree at Montana State University, I agree that the Library shall make it available to borrowers under rules of the Library. I further agree that copying of this thesis is allowable only for scholarly purposes, consistent with "fair use" as prescribed in the U.S. Copyright Law. Requests for extensive copying or reproduction of this thesis should be referred to University Microfilms International, 300 North Zeeb Road, Ann Arbor, Michigan 48106, to whom I have granted "the exclusive right to reproduce and distribute copies of the dissertation in and from microfilm and the right to reproduce and distribute by abstract in any format."

Signature John J. Golden

Date 21 June 1986

ACKNOWLEDGMENTS

The opportunity to perform the work supporting this thesis was the result of efforts from many good people, and I hope that all involved know of my gratitude. However, there are some to whom I am especially indebted. The project would not have occurred without the support and guidance of Dr. John Sears. Likewise, I would like to thank Dr. Doug Smith and all members of my research committee. Essential equipment was graciously provided by the MSU Chemistry Department and Dr. Frank Williams of the University of New Mexico. Financial support was, in part, provided by the Engineering Experiment Station and the Research Creativity Committee, both of MSU. I would like to thank my fellow graduate students and the staff of the Chemical Engineering Department for maintaining such a positive, constructive working environment. But foremost, I sincerely thank my wife, Linda Jean, for her love in support of this effort.

TABLE OF CONTENTS

Page

LIST OF TABLES vii

LIST OF FIGURES ix

ABSTRACT xv

I. INTRODUCTION 1

II. LITERATURE SURVEY 5

Catalytic Cracking Chemistry 5
Production of Silica-Alumina Catalysts 7
Measurement of Surface Acidity 10
    Titration Methods 10
    Gaseous Base Methods 15
    Infrared Spectroscopy Methods 18
    Catalytic Activity Methods 20
    Other Methods 24
Adsorption Site Energy Distributions on Heterogeneous Surfaces 26
Catalyst Morphology 31

III. EXPERIMENTAL 35

Synthesis and Preparation of Silica-Alumina Catalysts . . 35
Measurement of Water Loss 37
Measurement of Surface Area 38
Nonaqueous Titration 41
Measurement of Pore Volume Distribution and True Density 42
Measurement of Alumina Content 42
Chemisorption of Triethylamine 43
    Adsorption Apparatus 44
    Blank Measurements 49
    Experimental Method 50
    Calculations for TEA Adsorption Isotherms 54
    Calculations for the Application of the CAEDMON Program to TEA Adsorption Isotherms 56
Catalyst Activity Using Isomerization of o-Xylene . . . 61
    Reactivity Apparatus 62
    Blank Measurements 66
    Experimental Method 67
    Calculations 68

TABLE OF CONTENTS--Continued

Page

IV. RESULTS AND DISCUSSION 71

Preliminary Experiments 71
Synthesis and Preparation of the Silica-Alumina Materials 72
Chemical Composition of Catalysts 76
Water Loss 76
Alumina Content 78
Catalyst Morphology 82
Catalyst Surface Area 82
Catalyst Density 84
Catalyst Pore Volume 86
Chemisorption of Triethylamine 87
Acid-Site Strength Distributions 97
Catalyst Activity for o-Xylene Isomerization 104
Comparison of Acidity and Activity 116

V. CONCLUSIONS 121

VI. RECOMMENDATIONS FOR FURTHER STUDY 123

REFERENCES CITED 125

APPENDICES 130

Appendix A. Silica-Alumina Surface Structures 131
Appendix B. Surface Area Measurement 133
Appendix C. The CAEDMON Technique 138
Derivation of the CAEDMON Method 139
Estimation of Two-Dimensional Virial Coefficients . . . 156
Appendix D. Mercury Porosimetry Data and Calculations . 161
Appendix E. Calculation of TEA Diffusivity 186
Appendix F. Data for TEA Adsorption Isotherms 192
Appendix G. CAEDMON Results of Adsorption Energy Distributions 205
Appendix H. Reactor Tracer Experiment 216
Appendix I. Intraparticle Diffusion Criterion 219
Appendix J. o-Xylene Isomerization Equilibrium Limitations 222
Appendix K. Catalyst o-Xylene Isomerization Activity Data 224

LIST OF TABLES

Tables		Page
1.	Superacid solutions [6].	10
2.	Hammett acidity of several solids [4].	13
3.	Surface spectroscopies.	25
4.	Catalyst alumina compositions.	80
5.	Strong acid sites calculated by CAEDMON.	100
6.	Properties of strong acid sites.	103
7.	o-Xylene isomerization activity.	114
8.	Pore volume distribution calculations for sample A-0.	184
9.	Mercury porosimetry results.	185
10.	Blank experimental TEA adsorption data.	195
11.	TEA adsorption data for sample A-0 at ~300°C.	195
12.	TEA adsorption data for sample A-3 at ~200°C.	196
13.	TEA adsorption data for sample A-3 at ~300°C.	197
14.	TEA adsorption data for sample A-7 at ~300°C.	198
15.	TEA adsorption data for sample A-10 at ~300°C.	199
16.	TEA adsorption data for sample A-18 at ~300°C.	200
17.	Duplicate TEA adsorption data for sample A-18 @ ~300°C.	201
18.	TEA adsorption data for sample A-26 at ~300°C.	201
19.	TEA adsorption data for sample A-44 at ~300°C.	202
20.	TEA adsorption data for sample A-65 at ~300°C.	203
21.	TEA adsorption data for sample A-88 at ~300°C.	203
22.	TEA adsorption data for sample A-100 at ~300°C.	204

LIST OF TABLES--Continued

Tables Page

23. o-Xylene isomerization activity data for sample A-0. 225
24. o-Xylene isomerization activity data for sample A-3. 225
25. o-Xylene isomerization activity data for sample A-7. 226
26. o-Xylene isomerization activity data for sample A-10. 227
27. o-Xylene isomerization activity data for sample A-18. 228
28. o-Xylene isomerization activity data for sample A-26. 229
29. o-Xylene isomerization activity data for sample A-44. 230
30. o-Xylene isomerization activity data for sample A-65. 231
31. o-Xylene isomerization activity data for sample A-88. 231
32. o-Xylene isomerization activity data for sample A-100. 232

LIST OF FIGURES

Figures Page

1. Propylene polymerization versus acid amount for a series of silica-alumina catalysts [8]. 14

2. Correlation between catalyst activity (as measured by the temperature required for 25% conversion of o-xylene) and the Brønsted acidity of rare earth Y zeolites [31]. 19

3. Poisoning effect of amines on cumene cracking over silica-alumina catalyst [24].

4. Schematic diagram of the physisorption apparatus for the measurement of surface area. 39

5. Schematic diagram of the chemisorption apparatus for the measurement of triethylamine adsorption isotherms. 45

6. Front view of the chemisorption apparatus. 46

7. Left-side view of the chemisorption apparatus. 46

8. Schematic diagram of the reactivity apparatus. 63

9. Qualitative relationship of the moles of hydroxide ion required to form a pH 6 hydrogel versus the moles of aluminum ion contained in the reactant solution. 74

10. Thermogravimetric analysis for several of the silica-alumina xerogels, depicted as the percent of the original sample weight versus temperature. 77

11. Weight percent water loss as a function of expected alumina content for the xerogels. 79

12. Comparison of the expected and measured alumina contents of the catalysts. 81

13. Surface area versus measured alumina content. 83

LIST OF FIGURES--Continued

Figures Page

14. True density versus measured alumina content of the catalysts. 85

15. Adsorption isotherms for catalyst A-3, measured at two temperatures. 89

16. Adsorption isotherms for catalysts A-0, A-3, and A-7 at ~300°C. 91

17. Adsorption isotherms for catalysts A-10 and A-18 at ~300°C. 92

18. Adsorption isotherms for catalysts A-26 and A-44 at ~300°C. 93

19. Adsorption isotherms for catalysts A-65, A-88, and A-100 at ~300°C. 94

20. Test for the significance of external mass-transfer on reactivity measurements. 106

21. Test for the significance of internal mass-transfer on reactivity measurements. 108

22. First-order rate constant Arrhenius plot for catalysts A-3, A-7, and A-18. 109

23. First-order rate constant Arrhenius plot for catalysts A-10, A-26, and A-44. 110

24. Isomerization rate Arrhenius plot for catalysts A-3, A-7, and A-18. 111

25. Isomerization rate Arrhenius plot for catalysts A-10, A-26, and A-44. 112

26. Relationship of the strong acidity measured from chemisorption isotherms to the measured alumina contents of the catalysts. 117

LIST OF FIGURES--Continued

Figures Page

27. Relationship of the o-xylene isomerization rate at 300°C to the measured alumina contents of the catalysts. 118

28. Logarithm of the o-xylene isomerization rate shown as a function of the strong acidity of the catalysts. 120

29. Some proposed silica-alumina surface structures [6, 11, 14, 64]. 132

30. Physisorption apparatus blank response as observed weight loss vs. system pressure. 134

31. Program for the calculation of BET surface area. 135

32. Effect of variation in the second 2D virial coefficient on the calculated adsorption energy distribution using the data of Sacher and Morrison [44]. 142

33. Effect of variation in the third 2D virial coefficient on the calculated adsorption energy distribution using the data of Sacher and Morrison [44]. 143

34. Effect of combined variations in the second and third 2D virial coefficients on the calculated adsorption energy distribution using the data of Sacher and Morrison [44]. 144

35. Results of testing the CAEDMON program for the effect of variation in the number of surface adsorption patches on the computed adsorption energy distribution using the data of Sacher and Morrison [44]. 145

LIST OF FIGURES--Continued

Figures Page

36. Mercury penetration volume vs. pore radius for sample A-0. 162

37. Mercury penetration volume vs. pore radius for sample A-3. 163

38. Mercury penetration volume vs. pore radius for sample A-7. 164

39. Mercury penetration volume vs. pore radius for sample A-10. 165

40. Mercury penetration volume vs. pore radius for sample A-18. 166

41. Mercury penetration volume vs. pore radius for sample A-26. 167

42. Mercury penetration volume vs. pore radius for sample A-44. 168

43. Mercury penetration volume vs. pore radius for sample A-65. 169

44. Mercury penetration volume vs. pore radius for sample A-88. 170

45. Mercury penetration volume vs. pore radius for sample A-100. 171

46. Pore size distribution for sample A-0, calculated from the porosimetry data shown on Figure 36. 172

47. Pore size distribution for sample A-3, calculated from the porosimetry data shown on Figure 37. 173

48. Pore size distribution for sample A-7, calculated from the porosimetry data shown on Figure 38. 174

LIST OF FIGURES--Continued

Figures Page

49. Pore size distribution for sample A-10, calculated from the porosimetry data shown on Figure 39. 175

50. Pore size distribution for sample A-18, calculated from the porosimetry data shown on Figure 40. 176

51. Pore size distribution for sample A-26, calculated from the porosimetry data shown on Figure 41. 177

52. Pore size distribution for sample A-44, calculated from the porosimetry data shown on Figure 42. 178

53. Pore size distribution for sample A-65, calculated from the porosimetry data shown on Figure 43. 179

54. Pore size distribution for sample A-88, calculated from the porosimetry data shown on Figure 44. 180

55. Pore size distribution for sample A-100, calculated from the porosimetry data shown on Figure 45. 181

56. TEA adsorption isobars measured for samples A-3, A-7, A-18, and A-44. 193

57. TEA adsorption isobars measured for samples A-10, A-26, A-88, and A-100. 194

58. CAEDMON results for sample A-3. 206

59. CAEDMON results for sample A-7. 207

60. CAEDMON results for sample A-10. 208

61. CAEDMON results for sample A-18. 209

62. CAEDMON results for sample A-26. 210

63. CAEDMON results for sample A-44. 211

64. CAEDMON results for sample A-88. 212

LIST OF FIGURES--Continued

Figures Page

65. CAEDMON results for sample A-100. 213

66. CAEDMON results for the ammonia adsorption data of Hsieh [26]. 214

67. Natural gas (methane) tracer response of the Berty reactor, indicated by the logarithm of the natural gas concentration (GC peak area) versus time after tracer injection. 218

68. Conversion limits for xylene isomerization reactions calculated from thermodynamic equilibrium. 223

ABSTRACT

Surface heterogeneity of a catalyst can be described in terms of adsorption energy distribution. In the present study, acid-site adsorption energy distributions have been obtained for the amorphous silica-alumina system, with results compared to o-xylene isomerization activity.

Xerogels ranging in composition from pure silica to pure alumina were synthesized using reagents which avoid sodium contamination. Calcination at 500°C was performed prior to making physical property, chemisorption, and activity measurements.

Catalysts were tested for surface area, porosity, density, alumina content, and water loss. Results indicate that unusual materials have been synthesized in the 50-75% alumina composition range, materials with low surface areas despite having high initial water contents.

Triethylamine chemisorption isotherms were gravimetrically measured at ~300°C. The minimum adsorbate injection possible with the equipment used was not low enough to measure the very low coverage portion of the isotherms. The adsorption isotherms were analyzed with a recently-developed numerical technique known as CAEDMON (Computed Adsorption Energy Distribution in the MONolayer). The calculated quantities of strong acid sites for test catalysts was in general agreement with other chemisorption studies on comparable materials.

Catalyst activity for o-xylene isomerization was measured at 300-400°C using a Berty reactor. Reaction rates were obtained avoiding equilibrium and transport limitations. Activation energies of 17 to 21 kcal/mole were observed for reactive catalysts.

Reaction rates for low alumina-content catalysts were observed to be exponentially related to the quantity of strong acid-sites. Correction of intermediate alumina content catalysts for alumina-type acidity unreactive for o-xylene isomerization yielded acidities fitting the exponential relationship.

It is postulated that two major types of strong acid sites were observed for the silica-alumina catalysts, Brønsted acid sites active for isomerization and Lewis acid sites associated with alumina which are inactive for isomerization. The exponential relationship between the quantity of Brønsted sites and catalytic activity appears to indicate a proximity effect, such that acid-site reactivity increases as the distance between acid sites decreases.

I. INTRODUCTION

Silica-alumina is one of the most extensively studied solid systems. The volumes of research are certainly due to the development of cracking catalysts for the petroleum feedstock production of gasoline. Continuous improvement of cracking catalysts over the last 40 years has lead to the development of zeolites, crystalline aluminosilicates also called molecular sieves.

Though largely replaced by zeolites for catalytic cracking, amorphous silica-alumina is still used to support the expensive zeolite to better effect heat transfer. Silica-alumina can also act as a metallic catalyst support and be used as a bifunctional catalyst. Recently, interest in the preparation and characterization of amorphous silica-alumina has been cited because of the material's newly discovered capability for converting methanol into hydrocarbons [1]. But most importantly, the extensive background concerning silica-alumina makes the system ideal for the fundamental study of an amorphous solid surface. It is the fundamental study of solid surfaces that is of interest to several Chemical Engineering researchers at Montana State University.

Despite the years of research, amorphous silica-alumina materials exhibit properties that are not well understood. What follows here is a restatement of some of the observations made by reviewers [2-7] concerning the character of cracking catalysts.

Catalytic cracking has been previously defined as the set of hydrocarbon reactions that occur on acidic solids. These reactions include dealkylation, hydrogen transfer, isomerization, and polymerization.

In general, silica-alumina catalysts have been observed to exhibit adsorption sites suggesting Lewis and Brønsted acidity, as well as interconversion between the two types of sites. Due to observations consistent with carbonium ion chemistry, many investigators believe that the seat of catalytic cracking on silica-alumina is the Brønsted acid sites. However, some cracking reactions have been found to correlate with measurements of Lewis acidity.

Whether actual carbonium ion chemistry is occurring on cracking catalysts has been questioned. It is known that the forces bonding large cracking feedstock molecules to microporous surfaces are both physical and chemical. Such an interaction could promote a more concerted mechanism involving simultaneous bond breaking and bond formation. But at this time, it is not known if catalytic cracking reactions are being oversimplified when described as carbonium ion reactions.

Both Lewis and Brønsted acid sites on silica-alumina exhibit energetic heterogeneity, ranging from very weak acids (alcoholic) to very strong acids (superacids). The seldom-studied consequence of broad energetic heterogeneity is that the catalytic activity of these materials may be due as much to the acid-site strength distribution as to the total number of acid sites.

Measurements of some cracking reactions indicate a maximum silica-alumina catalyst activity at a bulk concentration of 15-25% alumina. However, a number of factors during synthesis, calcination, and pretreatment affect the catalyst surface. The relationship between bulk alumina composition and the corresponding surface structures is not well understood.

Research Objectives

It is the purpose of this research to contribute to the fundamental understanding of amorphous silica-alumina catalysts. The research objectives are:

1. To synthesize and physically characterize a composition range of amorphous silica-alumina materials. These catalysts will be synthesized such that contamination is avoided. Catalyst history will be entirely under the control of this research project.
2. To determine the acid-site energy distributions for the catalysts. Adsorption isotherms for a gaseous base adsorbate will be used to numerically calculate the expected heterogeneous adsorption energy distributions.
3. To compare the calculated energy distributions to catalytic cracking activity. The measure of cracking activity will be based on a well-studied model compound reaction.

A survey of the extensive literature concerning the acidity and characterization of silica-alumina catalysts will follow in Chapter II. Chapter III contains a description of the experimental equipment and methods used in this study. The results and their discussion are contained in Chapter IV. Conclusions of research findings comprise Chapter V. Finally, observations of a more hypothetical nature and recommendations for future research are located in Chapter VI.

II. LITERATURE SURVEY

Catalytic Cracking Chemistry

Petroleum refining performed before the discovery of cracking catalysts required the thermal cracking of heavy molecular weight feedstocks via free-radical mechanisms. There are several important consequences of the free-radical reaction. Paraffin radicals will frequently undergo scission, following the empirical β rule, to form ethylene and another primary radical. Hydrogen abstraction is another common hydrocarbon radical reaction. But isomerization involving alkyl group migration or shift of the radical along a hydrocarbon chain does not occur. As a result, thermal cracking of hydrocarbons from petroleum results in the formation of large amounts of ethylene from paraffins and in the dehydrogenation of naphthenes to aromatics [6].

Catalytic cracking reactions performed on acidic surfaces are believed to proceed via carbonium ion intermediates. This theory is primarily based on the similarities in product distribution found with heterogeneous cracking and cracking performed in mineral acid solution.

Organic chemists have thoroughly studied carbonium ion, sometimes called carbocation, reactions in solution and the reactivities of these species are well understood. In general, the carbonium ion intermediate is stabilized by the availability of electrons to the region of the ion. To a great extent, the stability of a carbonium ion determines its reaction pathway.

Carbonium ion formation reactions and mechanisms have been described in a detailed review of catalytic cracking by Gates et al. [6]. The formation of carbonium ions from hydrocarbons can occur: (1) via proton donation to olefins or aromatics by Brønsted acids, (2) via hydride abstraction from paraffins by Lewis acids, or (3) via protonation of paraffins by Brønsted acids to produce the carbonium ion and hydrogen. A secondary formation of carbonium ions, though not secondary in importance, can occur via hydride transfer (chain transfer).

Once carbonium ions are formed, they can undergo rearrangement (isomerization), polymerization (alkylation), or cracking (dealkylation). The mechanism of carbonium ion reactions is postulated as a transition through various three-centered electron deficient complexes, analogous to the electronic structures found in boranes.

The preponderance of product distribution data for catalytic cracking by acid surfaces leaves little doubt that the carbonium ion mechanism, as in solution, occurs on surfaces. However, the possibility of charge separation occurring on the catalytic surface, due to the immobility of the surface sites, has lead to speculation concerning the true degree of charge development occurring in reactant molecules. It has been suggested that carbonium ions may not actually be fully formed on the catalyst surface. Instead, the reactant molecules may become sufficiently polarized by the surface to react or rearrange through a more concerted mechanism before a carbonium ion could be formed. There is experimental evidence of such nonionic "intermediates" for some organic elimination reactions. However, it has been stated that there is currently insufficient information to determine if catalytic cracking reactions are oversimplified by being described as carbonium ion reactions [6].

Production of Silica-Alumina Catalysts

The commercial production of silica-alumina catalysts began in the 1940's with several companies holding patents to their manufacture. It is recognized that a number of interrelated variables, such as solids concentration, pH, temperature, and time, control the physical and chemical properties of the final catalyst [3]. Generally, commercial processes involve the acidification of dilute sodium silicate with sulfuric acid to form a silica hydrogel. Aluminum is added to the silica hydrogel as aqueous aluminum sulfate and hydrolysis (incorporation) is accomplished by the addition of aqueous ammonium hydroxide. Filtration is performed with water acidified to pH 4-5.5 to aid in sodium removal. Some manufacturing processes produce loosely packed, mostly spherical particles, 0.05-3 μm in diameter, that are then pressed together into regular pellets. Other processes produce a coarse grade of catalyst with a 60 μm average particle (clump) size.

Laboratory experiments involving cracking catalysts have largely used samples of commercial catalysts as the object of study. However, researchers wishing to vary the amount of alumina or to avoid the additional variable of sodium contamination in the catalyst have reported procedures for silica-alumina catalyst synthesis. A process described by Johnson [8] involved the interaction of a very pure silica gel, prepared at pH 3, with measured amounts of an alumina sol. The alumina sol was prepared from aluminum chloride, precipitated and thoroughly washed as the hydroxide, and then redissolved in water. The catalyst product was formed when the two components were mixed. The product was washed and then dried at 393 K.

Another laboratory process for silica-alumina synthesis was developed by Thomas [9]. A major objective of the process was to avoid sodium in the resulting product. This goal was accomplished by dissolving aluminum isopropoxide in tetraethyl orthosilicate (TEOS). The mixture was then hydrolyzed with water and ethanol.

More recently, a variety of approaches for the laboratory synthesis of silica-alumina have been reported [10-17]. One of these approaches, similar to the process by Thomas described previously, involved the formation of a silica hydrogel by reacting TEOS and hydrochloric acid at pH 2. Sufficient aluminum sulfate was dissolved in this mixture to give the chemical composition desired. Ammonia solution was then added to the mixture until it gelled at pH 6 [11].

The theory of how silicon and aluminum ions interact during the formation of active cracking catalysts has been discussed by several reviewers [2-6]. Commercial preparations generally start with the silica hydrogel, which consists of an aggregate of primary spherical particles about 30-50 Å in diameter. The primary particles consist of an interconnected network of SiO_4 tetrahedra, with the surface silicon ions terminated by hydroxyl groups. Next, an aluminum salt solution is added to the hydrogel. When the pH of the mixture is increased, the aluminum ions react with the silica surface hydroxyls. The result is that the trivalent, six-coordinate aluminum ions isomorphously substitute into the tetrahedral silica lattice. This incorporation of aluminum produces an active cracking catalyst, generally depicted as

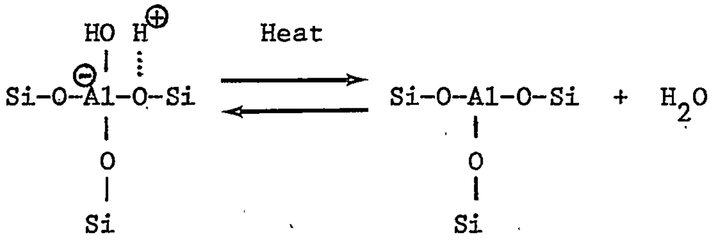

Brønsted Acid

Lewis Acid

Having both Brønsted and Lewis acid character is not unique to solid cracking catalysts. An analogous class of solutions is known to exhibit high proton donor strengths (superacids).

Table 1. Superacid solutions [6].

Brønsted Acid		Lewis Acid
H_2O	+	BF_3
HF	+	BF_3
HF	+	SbF_5
FSO_3H	+	SbF_5
HCl	+	$AlCl_3$

It is important to recognize that the above considerations are all simplified concepts of the very complicated cracking catalyst surface. The groups that actually exist could have varying degrees of aluminum incorporation or aluminum ion separation. Further treatment of cracking catalysts, such as calcination, will produce different surface structures. Other methods of silica-alumina preparation, each promoting different silica-alumina interactions, will produce still other surface structures. Some of the proposed silica-alumina surface structures are reproduced in Appendix A. However, the bulk structures and the corresponding surface structures of silica-alumina are not well known [6].

Measurement of Surface Acidity

Titration Methods

The observation that both silica-alumina catalysts and mineral acid solutions produced similar reaction products caused investigators to test silica-alumina catalysts in the aqueous phase with acid indicators. Once the catalyst surface was qualitatively observed as acidic [18], attention turned to obtaining more detailed information concerning this acidity and the chemical structure of the catalyst.

Early measurements of surface acidity continued to be performed in aqueous media. In essence, aqueous titration of surface acidity is an ion exchange process. Ion exchange measurements performed in the aqueous phase can provide some information concerning surface acidity. Good correlations of catalytic activity for acid reactions and ion exchange capacity based on the use of ammonium acetate have been reported [3]. However, titration with basic substances in aqueous solution was recognized as disadvantageous [3]. Not only will water react with the catalyst surface and alter its structure, but the acidity so determined will be limited by the acid strength of the hydronium ion.

The nonaqueous solution technique is performed using solvents such as benzene which do not react with the catalytic surface. A comparison of surface acid strengths in nonaqueous media can be based on the ability of the solid to change a neutral base into its conjugate acid form [7]. In this manner, as previously described by Hammett and Deyrup [19], acidity is defined by the function:

$$H_o = -\log \left[a_{H^+} \frac{\gamma_B}{\gamma_{BH^+}} \right] \qquad (1)$$

where

H_o = Hammett acidity function

a_{H^+} = proton activity

γ_B = neutral base activity coefficient

γ_{BH^+} = conjugate acid activity coefficient

The nonaqueous technique, using a series of aniline bases as indicators (Hammett indicators), has been employed to determine acid strengths for a variety of solids. The data in Table 2 was obtained by a nonaqueous indicator method and reported by Tanabe [4].

The nonaqueous indicator method is the simplest way of screening solid catalysts for surface acidity. However, several disadvantages to this method have been recognized. Numerous sources [4,5,7,20-22] have discussed the necessity of water being rigorously excluded, the importance of solvent choice, the sometimes difficult recognition of end-point in the presence of colored solids, and the long time required for equilibrium. In addition, the nonaqueous indicator method cannot be used for acidity determination under cracking reactions conditions nor can it distinguish between Lewis or Brønsted acid sites on the solid surface.

Table 2. Hammett acidity of several solids [4].

Acidic Solids	Ho
Original kaolinite	-3.0 to -5.6
Hydrogen kaolinite	-5.6 to -8.2
Original montmorillonite	+1.5 to -3.0
Hydrogen montmorillonite	-5.6 to -8.2
Silica-alumina	<-8.2
Silica-magnesia	+1.5 to -3.0
Alumina-boria	<-8.2
H_3BO_3/silica gel	+3.3 to +1.5
H_3PO_4/silica gel	+1.5 to -3.0
H_2SO_4/silica gel	-5.6 to -8.2
$HClO_4$/silica gel	-5.6 to -8.2

Although the nonaqueous titration technique has several recognized drawbacks, its use has been frequently reported in the literature. Cases of strong correlation between acidity via the indicator method and catalytic activity have been published. Johnson [8] titrated the total acidity of several silica-alumina compositions dispersed in benzene using n-butylamine as titer and p-dimethylaminoazobenzene (dimethyl yellow) as indicator. The total acidity so determined was observed to vary linearly with propylene polymerization activity as shown in Figure 1. It was also found that acidity and polymerization activity increased to a maximum value and then decreased with increasing alumina content.

An improved Hammett indicator technique, avoiding several of the disadvantages previously mentioned concerning the titration method, was reported by Benesi [21]. The technique avoided the problems of water exclusion and long equilibrium time. Several mounted acids, clays, and cracking catalysts were tested. Benesi observed that 90% of the acid centers on silica-alumina catalysts were very strong ($Ho < -8.2$).

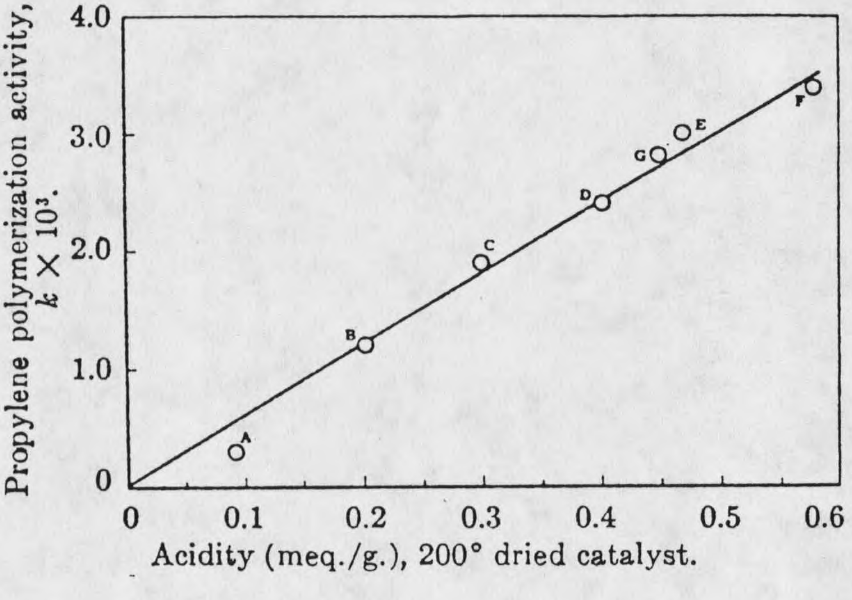

Figure 1. Propylene polymerization versus acid amount for a series of silica-alumina catalysts [8].

Catalyst:	A	B	C	D	E	F	G
Alumina:	0.12	0.32	1.04	2.05	3.56	10.3	25.1

Hammett indicators have since been obtained that extend the acid strength range of the n-butylamine titration method. These indicators are generally observed using absorption spectroscopy, which reduces the uncertainties inherent in visual observation. Using these improvements, Take et al. [23] found that the acid sites on a silica-alumina catalyst had an acid strength corresponding to an Ho between -10.5 and -12.8. A few sites had even higher acid strengths.

Another nonaqueous technique used to determine the acid amount of solids is the calorimetric titration. Temperature rise is recorded with the addition of measured amounts of a titrating base such as n-butylamine. The calorimetric titration has been used to observe both weaker acid sites than those found with indicators and energetic heterogeneity in the acid sites [4,5].

Gaseous Base Methods

The strength and number of acid sites can be more explicitly obtained by determining the amount of a gaseous base that will adsorb on an acidic solid. Gaseous bases such as ammonia, n-butylamine, pyridine, and quinoline have been adsorbed on cracking catalysts at temperatures similar to those used at reaction conditions. Of course, there is an upper limit to the adsorption temperature because gaseous bases will catalytically decompose. In addition, some gaseous bases can dissociate and consequently adsorb onto both acidic and basic sites. Since triethylamine (TEA) is very difficult to dissociate, it has been recommended to be used as an acid catalyst adsorbate [22].

Gaseous bases will also adsorb onto both Brønsted and Lewis acid sites, making it difficult to distinguish the amounts of each [5].

The classical study of cracking catalysts by Mills et al. [24] made use of the gravimetric determination of gaseous base adsorption. The study obtained a linear relationship between the amount of quinoline chemisorption and the light gas-oil cracking activity for a number of different cracking catalysts. However, the quinoline adsorption was not measured at accurately known equilibrium pressures.

Many other techniques using gaseous bases have been employed by researchers for the characterization of surface acidity. Calorimetric methods and the measurements of adsorption or desorption isotherms at several temperatures have enabled investigators to determinate the heat and entropy of adsorption for cracking catalysts as a function of surface coverage. Differential thermal analysis (DTA), thermal gravimetric analysis (TGA), and temperature programmed desorption (TPD) are similar methods that have been used to estimate the acid strengths of silica-alumina catalysts [4].

Ammonia gas TPD has been reported by Barth and Ballou [25] for several materials including silica-alumina catalysts. Total acid results were in general agreement with nonaqueous indicator measurements, but acid strength was discussed only qualitatively.

In the study by Hsieh [26], adsorption isotherms and calorimetric heats of adsorption were measured using ammonia at 273 K. Commercial cracking catalysts that were fresh, used, heat-deactivated and steam-deactivated were tested. The procedure of Adamson and Ling [27] was used to find site energy distributions. Results of this study indicated that there were two predominant site energies (acid strengths) on the catalysts. It was also observed that the highest energy sites were those lost in the three deactivated catalysts.

The adsorption of ammonia on eleven silica-alumina gels ranging in composition from pure silica to pure alumina was studied by Clark, et al. [28]. Adsorption data was experimentally determined as isobars at several different ammonia pressures. Data plotted as isotherms was found to fit the Freundlich equation for all but the two highest silica-content catalysts. Isosteric heats of adsorption were obtained from the integrated form of the Clausius-Clapeyron equation for constant surface coverage. The isosteric heat curves (energies) dropped very rapidly with increasing coverage for the silica gel and high silica adsorbents. Curves for alumina and high alumina adsorbents dropped more slowly with coverage. The isosteric heat curves for the intermediate compositions, 55-90% silica, reached the lowest values.

Clark and his coworkers also calculated the differential molar entropy of the adsorbed ammonia. They found that the intermediate compositions provided the highest entropies. The cited authors concluded that the strongest acid sites were Lewis acid in character and the high alumina content adsorbents contained mostly this type. The intermediate compositions contained many weak acid sites which were judged to be the protonic (Brønsted) acid sites. The entropy calculations indicated that adsorption on the weak sites of intermediate compositions produced adsorbed molecules with the greatest mobility. It was also found that the trend in adsorbate mobilities compared closely with measurements of o-xylene isomerization activity [10].

Infrared Spectroscopy Methods

Infrared spectroscopy, used in conjunction with gaseous base adsorption, has received considerable research attention in recent years due to its ability to distinguish between Lewis and Brønsted acid sites. For example, pyridine can coordinatively bond to Lewis acid sites or it can associate with Brønsted sites as the pyridinium ion. These two adsorbed species have different infrared absorption bands. The amount of either acid type can be determined from the absorption band intensities. Experimental difficulties associated with this technique are extensive sample preparation as well as complicated equipment requirements and operation.

The pioneering work utilizing infrared spectroscopy in the determination of silica-alumina surface acidity was performed by Mapes and Eischens [29] when they incorporated infrared spectroscopy with the chemisorption of ammonia. Though this work encountered significant experimental difficulties, the authors felt certain that they had observed both Brønsted and Lewis acids on the surface of a silica-alumina catalyst, and that most of the acid sites were of the Lewis type.

The use of pyridine rather than ammonia for infrared studies of chemisorbed bases was suggested by Parry [30]. The pertinent pyridine absorption bands are well separated and removed from possible interference with bands arising from water or surface hydroxyls.

Research reported by Ward and Hansford [31] has made use of the infrared spectrum of chemisorbed pyridine. A linear relationship was observed between the amount of Brønsted acid (peak height/sample mass) and the temperature required for an o-xylene isomerization conversion of 25% (See Figure 2), using a zeolite catalyst. A similar study by Schwarz [17] using silica-alumina catalysts of varying silica content measured Brønsted acid site concentrations in good agreement with previously reported activities for the isomerization of o-xylene over similar silica-alumina catalysts [10].

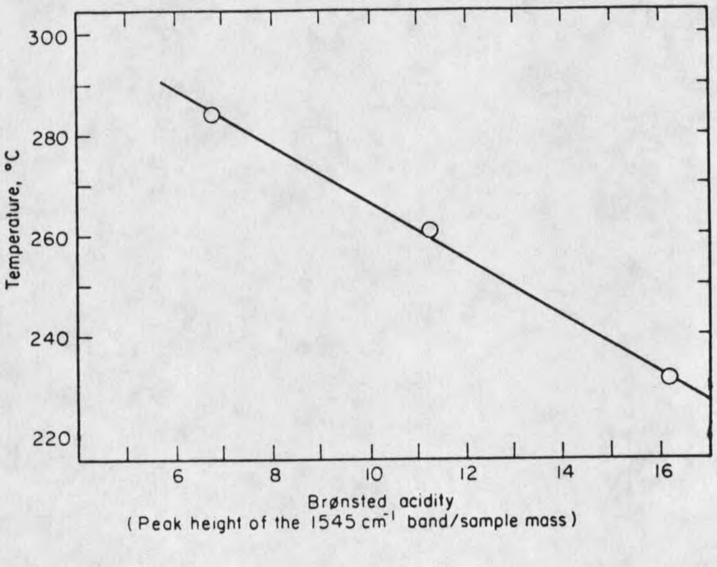

Figure 2. Correlation between catalyst activity (as measured by the temperature required for 25% conversion of o-xylene) and the Brønsted acidity of rare earth Y zeolites [31].

Infrared measurements of chemisorbed pyridine was also tried by Bourne et al. [11] as a way of identifying acid sites on two types of silica-aluminas. The two catalysts consisted of low concentrations (< 1.4 wt.%) of aluminum atoms incorporated on the surface of silica gel or within the silica framework. It was found that dehydrated alumina-on-silica contained only Lewis sites and that dehydrated alumina-in-silica contained only Brønsted acid sites. Addition of water to dehydrated alumina-on-silica converted part of the Lewis acid sites to Brønsted acid sites.

Another infrared study of the interrelationship of silica-alumina acidity and activity for olefin polymerization was performed by Mizuno et al. [32]. From the results of their experiments, the authors found that strong Lewis acid sites (25-30% of the total Lewis acid content) were active for olefin polymerization on silica-alumina.

Catalytic Activity Methods

The primary objective of the various techniques for the characterization of surface acidity thus far described was practical correlation with catalytic activity. For this reason, numerous approaches have been developed to infer surface structures from catalytic activity measurements. One technique, generally described as catalytic titration, involved monitoring a catalytic reaction while a known amount of catalyst poison was introduced into the system. Another technique made use of model compounds which required different acid types or strengths for reaction to occur. Although techniques of these types would seem to provide the most relevant information, interpretation of data usually required the use of a supportive technique, like those previously described, for complete analysis.

When a catalyst poison is gradually introduced into an acid catalyst system, it will primarily interact with the most acidic (highest energy) sites on the surface. As a result, reactions requiring the highest acid strength will be inactivated first. If the catalyst poisoning continues, progressively weaker acid-catalyzed reactions will be inactivated. Silica-alumina gradually poisoned by pyridine has shown the following reactions have decreasing acid strength requirements [7].

1. Skeletal isomerization of isobutylene to n-butenes
2. Dealkylation of tert-butylbenzene (cracking)
3. Double bond migration and trans-cis isomerization of n-butenes
4. Depolymerization of diisobutylene to butenes
5. Dehydration of tert-butanol to butenes

Effects of partial quantitative poisoning were investigated by Mills et al. [24] by determining the catalytic cracking of cumene over silica-alumina pretreated with various amounts of nitrogenous bases. Results indicated that the amount of poison adsorbed by the catalyst was exponentially related to the weight percent benzene in the product stream. Base poisoning effectiveness was reported as being due to the basicity and thermal stability of the nitrogen bases. However, it also seems to be related to steric hindrance of the acid site, decreasing in the order : quinaldine > quinoline > pyrrole > piperidine > decylamine > aniline (See Figure 3).

A similar catalytic titration was carried out by Parera [33]. It was found that n-butylamine was 10 times as effective a catalyst poison as sodium, again possibly indicating a steric effect.

Using a model compound for the determination of dealkylation activity on cracking catalysts was the method investigated by Johnson and Melik [34]. The dealkylation of tert-butylbenzene was reported to be catalyzed only by Brønsted acids. Therefore, the Brønsted activity of the catalyst could be determined directly from dealkylation activity. These researchers observed a loss of dealkylation activity with catalyst dehydration and found no correlation between dealkylation activity and nonaqueous titration (Hammett) method.

As previously stated, the stability of a carbonium ion determines its reaction pathway, indeed whether or not the ion will actually be formed. Studies by Andreau et al. [12] and Sugioka and Aomura [35] have made use of the known order of alkyl carbonium ion stability for the investigation of silica-alumina catalysts. Cracking activity of isomeric butylbenzenes follows the order expected when reaction occurs via carbonium ion intermediates. This is in agreement with other studies correlating catalytic activity and Brønsted acidity.